Enhancement of the Wolf Damped Coulomb Potential: Static, Dynamic, and Dielectric Properties of Liquid Water from Molecular Simulation

Dirk Zahn,† Bernd Schilling, and Stefan M. Kast*

Institut für Physikalische Chemie, Technische Universität Darmstadt, Petersenstrasse 20, 64287 Darmstadt, Germany

Received: April 17, 2002; In Final Form: July 18, 2002

The recently introduced damped Coulomb potential [Wolf, D.; Keblinski, P.; Phillpot, S. R.; Eggebrecht, J. *J. Chem. Phys.* **1999**, *110*, 8254] is analyzed and slightly modified to obtain a significant improvement of dielectric properties when applied to simulations of dipolar liquids. It is used in molecular dynamics simulations of TIP3P and SPC water models. The results are compared with simulations using Ewald summation and the CHARMM shifted-force potential. A transferable scheme for parametrization of damping constants and cutoff radii is given. With a cutoff distance of only 9 Å, static properties such as average potential energy, particle density, and radial distribution functions, dynamic properties such as velocity autocorrelation function and dipole moment relaxation, and the dielectric constant are found to be in good agreement with the reference Ewald simulations.

I. Introduction

In molecular dynamics (MD) and Monte Carlo (MC) simulations, the accurate evaluation of electrostatic interactions is generally the computationally most demanding task. Several methods have been developed for the treatment of long-range nonbonded interactions. Ewald summation[1] is accepted as the most adequate treatment of Coulomb interaction in periodic systems. Besides reaction field techniques,[2,3] spherical cutoff methods[4] in which interactions are taken into account only within a sphere of a certain cutoff radius are computationally less-expensive and therefore widely used. It is well-known that a discontinuous truncation of the electrostatic potential at the cutoff distance introduces severe truncation artifacts.[5] Truncation errors may be reduced by the use of *switching* or *shifting* schemes. Switching functions that smooth a potential to zero over a certain interval are known to lead to unrealistic fluctuations of the effective molecular pair potentials near the cutoff distance. The best compromise so far seems to be a continuous shifting of the potential at all distances such that value *(shifted potential*) or value and first derivative of the potential both become zero at the cutoff distance (*shifted-force potential*), as implemented for instance in the commonly used CHARMM program.[6] An improved shifted-force potential, particularly with respect to the forces as used in MD simulations has been proposed by Schrimpf et al.[7] Both the functional form and the cutoff distance, as well as the methodology (atom-based or group-based truncation schemes), influence the quality of the approximation to the real long-range interactions. Several comparative studies have critically examined the various schemes with respect to different observables.[4,8,9]

Recently, Wolf et al.[10] investigated the origin of cutoff artifacts. In their clear analysis, they first showed that the cutoff artifacts are related to the existence of net charges within the cutoff spheres caused by the finite number of interaction sites considered. In the second step, it was demonstrated that shifting the potential by a neutralizing term corresponding to the net charge results in faster convergence to the Madelung limit. Ultimately, they came up with an expression for a damped Coulomb potential satisfying the requirements of charge neutrality and force shifting for use in MD simulations. Physically interpreted, the effective Coulomb interaction in a polarizable medium was shown to decay as the inverse fifth power of the distance[11] so that the existence of net charges leads to considerably longer-ranged behavior explaining a large portion of the artifacts. Moreover, in molecular simulations using conventional shifted-force schemes, particles penetrate the cutoff sphere and instantly change the net charge. This is effectively circumvented by damping the potentials such that interactions are switched on and off more smoothly.

In light of the exceptional success of the damping scheme in their simulations of simple ionic systems even for small cutoff radii,[10] it appeared promising to apply the methodology to molecular systems. Demontis et al.[12] quite recently used the original form of the damped Coulomb potential in a simulation study of liquid water and anhydrous and hydrated aluminosilicates and discussed criteria for the selection of proper combinations of the damping parameters. With their final set, a significant speed-up compared to the traditional Ewald scheme could be achieved.

As has been noted in Wolf et al.'s original work, the forces and potentials are not consistent. In this work, we remove the inconsistency yielding a significant improvement of dielectric properties when applied to dipolar liquids. For evaluation of this enhanced potential, we focus in this article on simulations of pure liquid water with the commonly used TIP3P[13] and SPC[14] water models. The performance of the enhanced damped Coulomb scheme is compared with benchmark Ewald simulations and the conventional CHARMM cutoff method. The paper is organized as follows: In section II, the basic theory is described and the consistent formulation for potential and force is given along with a discussion of the dielectric properties. In

* To whom correspondence should be addressed. E-mail: kast@pc.chemie.tu-darmstadt.de. Telephone: +49 6151 165397. Fax: +49 6151 164298.

† Present address: Max-Planck-Institut für Chemische Physik fester Stoffe, Nöthnitzerstrasse 40, 01187 Dresden, Germany.

10.1021/jp025949h CCC: $22.00
Published on Web 09/21/2002

the following section, we describe a pragmatic strategy for parametrization of damping constants and cutoff radii to achieve simulation results of near Ewald quality. In section IV, static, dynamic, and dielectric properties as obtained from MD simulations with the various Coulomb summation schemes are reported. In the final section, our results are summarized.

II.Theory

(a) The Enhanced Damped Coulomb Potential. The derivation of the damped Coulomb potential was given by Wolf et al.[10] for purely ionic systems. We shall summarize this formalism and extend it to molecular sytems. The total Coulomb energy in units of 4π times the vacuum dielectric constant for an ion i is given by

$$E_i^{\mathrm{tot}}(r_{ij}) = \sum_{j\neq i} \frac{q_i q_j}{r_{ij}} \tag{1}$$

where q_i is the charge of ion i and q_j is the charge of another ion j at distance r_{ij}. In practice, the evaluation of the infinite sum has to be approximated by a finite sum. This may be done either by introducing periodicity and performing Ewald summation or by considering only ions j that are within a cutoff sphere of radius R_C. Equation 1 is then approximated by

$$E_i^{\mathrm{tot}}(r_{ij}) \approx \sum_{\substack{j\neq i \\ r_{ij}<R_C}} \frac{q_i q_j}{r_{ij}} \tag{2}$$

It is well-known that this radial summation of truncated potentials does not converge to the true limit. Even for large cutoff radii, evaluation of eq 2 leads to dramatic errors. Wolf et al.[10] have shown that this error is related to the existence of a net charge within the cutoff sphere. Thus, the accuracy may be significantly improved by introducing a correction term, E_i^{neutral}, that compensates for the lack of charge neutrality in the truncated sum in eq 2. The error in evaluating the total Coulomb energy is then of the order R_C^{-2}:

$$E_i^{\mathrm{tot}}(r_{ij}) = \sum_{\substack{j\neq i \\ r_{ij}<R_C}} \frac{q_i q_j}{r_{ij}} - E_i^{\mathrm{neutral}} + O(R_C^{-2}) \tag{3}$$

For ionic crystals, E_i^{neutral} may be determined in the following way: The ions are grouped as charge-neutral "molecules". For a simple crystal of only two species, A^+ and B^-, these "molecules" are most simply chosen as dipoles containing one ion of each species at minimum distance. The sum of Coulomb potential terms is now taken for those ions only that belong to "molecules" that are entirely within the cutoff sphere, yielding a "charge-neutralized" summation of interaction terms. E_i^{neutral} is given by the difference of the sum according to eq 2 and the "charge-neutralized" sum of the Coulomb potential.

Wolf et al.[10] derived an elegant method to approximate E_i^{neutral}. Let the maximum ion distance within a charge-neutral group be b. All ions j that belong to "molecules" truncated by the cutoff sphere are within a distance $R_C - b < r_{ij} < R_C + b$ to ion i. If b is small compared to the cutoff radius, the Coulomb interaction of the truncated "molecules" becomes approximately

$$E_i^{\mathrm{neutral}} \approx \sum_{j'} \frac{q_i q_{j'}}{R_C} = \frac{q_i \Delta q_i}{R_C} \tag{4}$$

where the prime on the index j indicates summation over ions belonging to truncated "molecules" only and Δq is the net charge within the cutoff sphere. With the use of this approximation, the total Coulomb energy for a configuration $\mathbf{r}$ is given by

$$E^{\mathrm{tot}}(\mathbf{r}) \approx \frac{1}{2}\sum_{\substack{i,j\neq i \\ r_{ij}<R_C}} \frac{q_i q_j}{r_{ij}} - \frac{1}{2}\sum_i \frac{q_i \Delta q_i}{R_C} = \frac{1}{2}\sum_{i,j\neq i} V^{\mathrm{sh}}(r_{ij}) \tag{5}$$

with the shifted pair potentials

$$V^{\mathrm{sh}}(r_{ij}) = \begin{cases} \dfrac{q_i q_j}{r_{ij}} - \dfrac{q_i q_j}{R_C} & \leftrightarrow \; r_{ij} < R_C \\ 0 & \leftrightarrow \; \text{else} \end{cases} \tag{6}$$

Although the summation in eq 4 is performed over truncated "molecules" only, the corresponding sum over the charge-neutral sites within a sphere exactly cancels to zero. Accordingly, the j sum in eq 5 can be done over all ions.

The shifted pair potential continuously reaches zero at the cutoff radius. In molecular dynamics simulations, it is necessary to use potentials of which the first derivatives also satisfy this condition. This may be accomplished by using shifted-force potentials. Wolf et al.[10] made an attempt to derive a shifted force from the potential eq 6 directly. This was achieved by a questionable operation in which differentiation and taking the limit are illegitimately assumed to commute:

$$\frac{\partial}{\partial r_{ij}} V^{\mathrm{sh}}(r_{ij}) = -\frac{q_i q_j}{r_{ij}^2} - \frac{\partial}{\partial r_{ij}}\frac{q_i q_j}{R_C} = -\frac{q_i q_j}{r_{ij}^2} - \frac{\partial}{\partial r_{ij}} \lim_{r_{ij}\to R_C} \frac{q_i q_j}{r_{ij}} \neq -\frac{q_i q_j}{r_{ij}^2} - \lim_{r_{ij}\to R_C} \frac{\partial}{\partial r_{ij}} \frac{q_i q_j}{r_{ij}} \tag{7}$$

From a physical point of view, it is reasonable to demand that all magnitudes such as potential, force, and higher derivatives become zero at R_C, avoiding a truncation. Mathematically, this would mean either a function that is zero everywhere or a function that is not analytic. Neither option is physically plausible, so using the shifted potential (eq 6) in a strict sense implies forces that, if required to be zero at R_C as well, are not consistent with the potential. Alternatively, we might view the formally constant R_C-dependent shifting terms as the result of an approximate average of contributions from many distances. In this way, the shift would be interpreted as an r-dependent variable thus validating the formal differentiation procedure. One can of course write down an expression for an *approximate* force according to the prescription of eq 7 and *enforce* consistency with the potential. In the present work, we therefore use a shifted-force potential that is derived from integration of the shifted force. Proceeding in this way is essential for the dielectric properties of dipolar liquids as shown later. Although the intuitive physical meaning of the charge neutralization is lost, our approach appears to be an acceptable compromise if the original potential is not changed too much.

In practical work, it is advantageous to use Wolf et al.'s damping approach. One has to make a compromise between the absence of truncation effects and the deformation of the original pair potential. Wolf et al.[10] found an elegant way to combine their results of the charge neutralization analysis with the idea of a damping function, $d(r_{ij})$, as a factor to the pair potential. Though the derivatives do not exactly reach zero, they may be damped closely to zero. The total energy of ion i reads

$$E_i^{\mathrm{tot}} = \sum_{j\neq i}\frac{q_i q_j}{r_{ij}} d(r_{ij}) + \sum_{j\neq i}\frac{q_i q_j}{r_{ij}}[1 - d(r_{ij})] \tag{8}$$

which formally resembles the Ewald summation procedure. Consequently, Wolf et al.[10] decided to use the error function complement $\mathrm{erfc}(\alpha r_{ij})$ as damping function, though the choice of $d(r_{ij})$ is somewhat arbitrary. Here, α is a damping parameter chosen in accordance with the cutoff radius R_C. By adding and subtracting the self-term associated with the second contribution

$$E_{\mathrm{self}} = \lim_{r_{ij}\to 0}\left\{\frac{1}{2}\sum_i \frac{q_i^2}{r_{ij}}\,\mathrm{erf}(\alpha r_{ij})\right\} = \frac{\alpha}{\pi^{1/2}}\sum_i q_i^2 \tag{9}$$

one obtains

$$E^{\mathrm{tot}} = \frac{1}{2}\sum_{i,j\neq i}\frac{q_i q_j}{r_{ij}}\,\mathrm{erfc}(\alpha r_{ij}) - \frac{\alpha}{\pi^{1/2}}\sum_i q_i^2 + \frac{1}{2}\sum_{i,j}\frac{q_i q_j}{r_{ij}}\,\mathrm{erf}(\alpha r_{ij}) \tag{10}$$

where now the last term can be shown to be very small[10] and negligible.

For a truncated potential, applying the charge neutralization procedure [cf. eqs 4 and 5] finally yields

$$E^{\mathrm{tot}} \approx \frac{1}{2}\sum_{\substack{i,j\neq i\\ r_{ij}<R_C}}\left(\frac{q_i q_j}{r_{ij}}\,\mathrm{erfc}(\alpha r_{ij}) - \frac{q_i q_j}{R_C}\,\mathrm{erfc}(\alpha R_C)\right) - \left(\frac{1}{2R_C}\,\mathrm{erfc}(\alpha R_C) + \frac{\alpha}{\pi^{1/2}}\right)\sum_i q_i^2 \tag{11}$$

The last term in eq 11 is now a self-energy associated with each ion *i*. Using the formally incorrect prescription (eq 7) for the derivation of damped Coulomb pair forces then gives[10]

$$F^{\mathrm{dc}}(r_{ij}) = \begin{cases} q_i q_j\left\{\dfrac{\mathrm{erfc}(\alpha r_{ij})}{r_{ij}^2} + \dfrac{2\alpha}{\pi^{1/2}}\dfrac{\exp(-\alpha^2 r_{ij}^2)}{r_{ij}} - \left[\dfrac{\mathrm{erfc}(\alpha R_C)}{R_C^2} + \dfrac{2\alpha}{\pi^{1/2}}\dfrac{\exp(-\alpha^2 R_C^2)}{R_C}\right]\right\} & \leftrightarrow\ r_{ij} < R_C \\ 0 & \leftrightarrow\ \text{else} \end{cases} \tag{12}$$

For molecular liquids consisting of neutral molecules without internal Coulombic interaction, the ions are replaced by the atomic sites and the ionic charges by partial charges. In this case, the self-term of eq 11 cancels, and it is safe to compute the interaction potential consistently by integrating the pair force, yielding

$$V^{\mathrm{dc}}(r_{ij}) = \begin{cases} q_i q_j\left\{\dfrac{\mathrm{erfc}(\alpha r_{ij})}{r_{ij}} - \left[\dfrac{\mathrm{erfc}(\alpha R_C)}{R_C^2} + \dfrac{2\alpha}{\pi^{1/2}}\dfrac{\exp(-\alpha^2 R_C^2)}{R_C}\right](r_{ij} - R_C)\right\} & \leftrightarrow\ r_{ij} < R_C \\ 0 & \leftrightarrow\ \text{else} \end{cases} \tag{13}$$

This relation constitutes the enhanced damped Coulomb potential. In the case of charged solutes, a modified expression for the self-term must be added to give the best approximation to full Ewald summation. Here, we only treat pure liquids that are simulated with the damped Coulomb formulas eqs 12 and 13.

The limiting factor in using the damped Coulomb scheme is the maximum atom distance within a molecule. As was shown above, eq 5 is valid only if this distance is small compared to the cutoff radius. For small molecules such as water, this condition is satisfied even better than for ionic systems. Larger molecules instead require larger cutoff radii or alternatively the introduction of charge-neutral subgroups within the entities.

(b) Dielectric Properties. The basic theory for treating dielectric properties in systems with toroidal boundary conditions was presented by Neumann and Steinhauser[15,16] almost two decades ago. The relative dielectric permittivity, ϵ_r, is given by the fluctuation formula

$$\frac{\epsilon_r - 1}{\epsilon_r + 2} = \frac{4\pi}{3}\frac{\langle M^2\rangle}{3Vk_BT}\left[1 - \frac{3}{4\pi}\frac{\epsilon_r - 1}{\epsilon_r + 2}\tilde{T}(0)\right] \tag{14}$$

where $\langle M^2\rangle$ is the fluctuation of the total dipole moment, k_B is the Boltzmann constant, T is the absolute temperature, and V is the volume of the basic cell. For a spatially isotropic system, $\tilde{T}(0) \equiv \tilde{T}_{xx}(0) = \tilde{T}_{yy}(0) = \tilde{T}_{zz}(0)$ denotes the $\mathbf{k} = 0$ limit of the Fourier transform (i.e., the integral) of the dipolar tensor $\mathbf{T}$ representing the effective interaction $-\boldsymbol{\mu}\cdot\mathbf{T}\cdot\boldsymbol{\mu}$ between molecular dipoles $\boldsymbol{\mu}$ in Gaussian units. For the general case of a radially symmetric damping function, $f(r)$, acting multiplicatively on the original Coulomb r^{-1} potential, we have to evaluate the $\mathbf{T}$ tensor elements

$$T_{ab} = \nabla_a\nabla_b(r^{-1}f(r)), \quad a,b \in \{x,y,z\} \tag{15}$$

One obtains after some algebra

$$\mathbf{T} = \mathbf{T}^0\left(f - r\frac{\mathrm{d}f}{\mathrm{d}r} + \frac{1}{3}r^2\frac{\mathrm{d}^2 f}{\mathrm{d}r^2}\right) + \frac{1}{3}r^{-1}\frac{\mathrm{d}^2 f}{\mathrm{d}r^2}\mathbf{I} \tag{16}$$

with $\mathbf{I}$ being the identity matrix; $\mathbf{T}^0$ is the dipolar tensor for a pure Coulomb potential. Considering the integral over the volume, the first term in eq 16 vanishes due to angular symmetry.[15] The only nonzero contribution to $\tilde{T}(0)$ comes from the second term:

$$\frac{4\pi}{3}Q \equiv \tilde{T}(0) = \int_V \mathrm{d}\mathbf{r}\left(\frac{1}{3}r^{-1}\frac{\mathrm{d}^2 f}{\mathrm{d}r^2}\right) = \frac{4\pi}{3}\int_0^{R_C}\mathrm{d}r\, r\frac{\mathrm{d}^2 f}{\mathrm{d}r^2} \tag{17}$$

Here, it is assumed that the molecular diameter is small compared with the cutoff distance as required by the damped Coulomb model. $Q = 1$ for Ewald summation represents the ideal infinite box size limit; any smaller value influences the dielectric constant.[15]

Turning now to the special cases of the original and the enhanced damped Coulomb potentials, we get from eq 17 and the damping term $f(r) = \mathrm{erfc}(\alpha r) - \mathrm{erfc}(\alpha R_C)$

$$Q^{\mathrm{dc,orig}} = \mathrm{erf}(\alpha R_C) - 2\alpha R_C\pi^{-1/2}\exp(-\alpha^2 R_C^2) \tag{18}$$

which evaluates to 0.9095 for a typical combination of $\alpha = 0.2$ Å^{-1} and $R_C = 9$ Å. This result would also be obtained with a truncated Ewald scheme. In contrast, the enhanced form, eq 13, yields

$$Q^{\mathrm{dc,enhanced}} = \mathrm{erf}(\alpha R_C) + \mathrm{erfc}(\alpha R_C) = 1 \tag{19}$$

TABLE 1: Geometric and Force Field Parameters for SPC and TIP3P Water Models[a]

	SPC	TIP3P
r_{OH} (Å)	1.000	0.9572
r_{HH} (Å)	1.633	1.5139
q_O (e)	−0.82	−0.834
q_H (e)	0.41	0.417
ϵ_O (kcal mol^{-1})	0.1554	0.1521
ϵ_H (kcal mol^{-1})	0	0
σ_O (Å)	3.166	3.150
σ_H (Å)	0	0

[a] r = distances; q = partial charges; ϵ and σ are Lennard-Jones parameters.

independent of α and R_C. Removing the inconsistency between force and potential by a simple shifted-force technique obviously improves the dielectric properties significantly compared to the original form.

III. Methods

(a) Simulation Conditions. Molecular dynamics simulations have been performed using a code developed in the group and the DL_POLY software.[17] Both SPC[14] and TIP3P[13] water models were investigated. Force field parameters and geometry of the water models are summarized in Table 1. Internal coordinates were constrained with SHAKE algorithm.[18] The simulation systems each contained 1000 water molecules with periodic boundaries applied to rectangular cells.

Reference data was obtained from MD simulations with Ewald summation using a real space cutoff of 12 Å and a Ewald coefficient chosen as 0.3 Å^{-1}. For each system, the initial equilibration and the determination of static observables were performed under *NpT* conditions[19−21] with the temperature set to 300 K and the pressure to 1 bar. In both models, a time step of 2 fs was applied. In addition to the damped Coulomb potential, the CHARMM shifted-force potential[6]

$$V_{\mathrm{CHARMM}}^{\mathrm{shf}}(r_{ij}) = \begin{cases} \dfrac{q_i q_j}{r_{ij}}\left[1 - \left(\dfrac{r_{ij}}{R_C}\right)^2\right]^2 & \leftrightarrow \; r_{ij} < R_C \\ 0 & \leftrightarrow \; \text{else} \end{cases} \quad (20)$$

was used for comparison.

When investigating dynamical properties, it is useful to switch to a microcanonical ensemble because the constant temperature and pressure algorithms have a significant effect on the system dynamics. The transition to *NVE* simulation was accomplished by first determining the average box volume and potential energy in *NpT* simulations. The *NpT* simulation run was stopped at a time when the box volume was equal to its average by a relative accuracy of 10^{-4}. Starting from this configuration, a *NVT* ensemble was simulated. This simulation was stopped as soon as the instantaneous potential energy reached its average value within the same accuracy. This procedure leads to well-defined systems for subsequent microcanonical simulations.

All systems were equilibrated for at least 200 ps. Static properties were computed from 200 ps sampling runs and dynamic properties from 2 ns simulations except for the diffusion coefficients for which short 20 ps runs were used (see below).

(b) Parametrization of the Damped Potential Parameters. In contrast to Demontis et al.[12] in which a general relation for an optimal parameter combination was sought on the basis of fixed box lengths, we here used a simple two-step strategy for finding a suitable combination of the damped potential parameters α and R_C in liquid systems with variable shape:

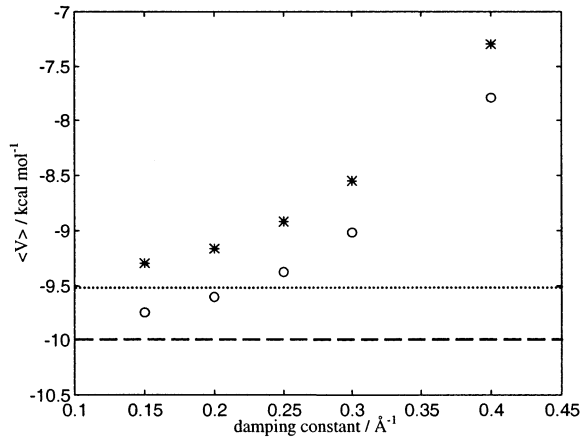

Figure 1. Average potential energy per water molecule for (○) SPC and (∗) TIP3P models. Ewald summation yields −10.00 kcal/mol (dashed) and −9.51 kcal/mol (dotted) for SPC and TIP3P water, respectively.

(i) At a given cutoff radius, *NpT* simulations were run for a range of damping constants. The initial cutoff radius was chosen to be the same as the real space cutoff radius of the Ewald simulations. The damping constant was varied from 0.15 to 0.4 Å^{-1}. For later cutoff reduction, it is favorable to choose the damping constant as large as possible. However, for both TIP3P and SPC water, the average potential energy and the density deviates increasingly from the reference values with larger damping constants. To ensure a simulation of near-Ewald quality, the damping constant was chosen such that the average potential energy per molecule and the average density did not deviate more than 5% from the values of the reference simulation. For both SPC and TIP3P water models, a reasonable α value was found to be 0.2 Å^{-1}. During the next step, the damping constant was kept fixed at this value.

(ii) In a new series of *NpT* simulations, the cutoff radii were varied from 12 to 6 Å. Again the resulting average potential energy and density were compared with the Ewald simulations. For a cutoff radius of 9 Å and larger, both properties were found to be within the desired agreement of 5% with the reference data. Thus, we chose the combination of α = 0.2 Å^{-1} and R_C = 9 Å for the simulation of SPC and TIP3P water at near-Ewald quality. The original and the enhanced damped Coulomb potential with these parameters are visually practically undistinguishable. Stronger deviations occur for much smaller values of α at the given R_C. It is interesting to note that our optimal result corresponds roughly to an estimate of α = 0.22 Å^{-1} along the lines of ref 12.

The optimal parameter combination was selected under constant pressure conditions because of the practical significance for the simulation of solutions in which a specific constant bulk water density is difficult to attain. For these problems, a pragmatically chosen parameter set determined for the pure solvent is sufficient and would be used for solutions without change.

IV. Simulation Results and Discussion

(a) Static Properties. To elucidate general trends, both water models, TIP3P and SPC, were simulated under *NpT* conditions using the damped potential with cutoff radius of 12 Å and the damping constant α varying from 0.15 to 0.4 Å^{-1}. Figures 1 and 2 show average potential energy and average density as a function of α. With increasing damping constant, both properties systematically deviate from the Ewald reference data. This is

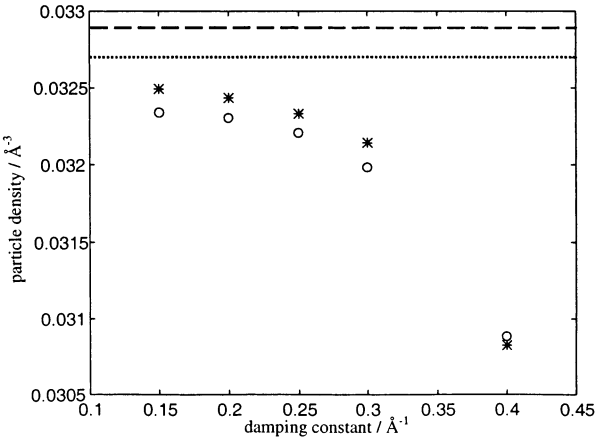

Figure 2. Average density of water molecules for (○) SPC and (∗) TIP3P models. Ewald summation yields 0.0329 Å^{-3} (dashed) and 0.0327 Å^{-3} (dotted) for SPC and TIP3P water, respectively.

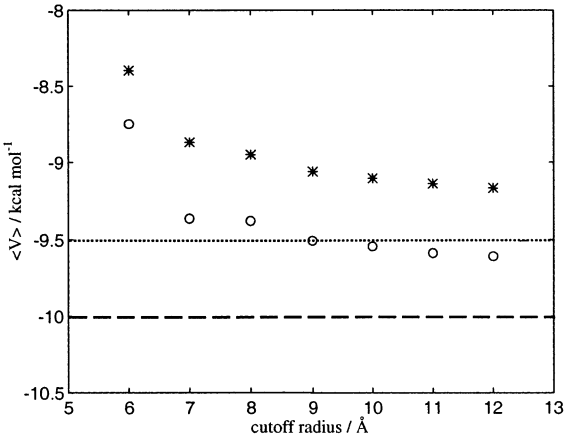

Figure 3. Average potential energy per water molecule as a function of the cutoff radii for (○) SPC and (∗) TIP3P models. Ewald summation yields −10.00 kcal/mol (dashed) and −9.51 kcal/mol (dotted) for SPC and TIP3P water, respectively.

readily explained by the damping of the Coulomb potential. The long-range interaction of the water molecules is dominated by dipole−dipole attraction. Thus the damping leads to an underestimation of the attractive part of the intermolecular interaction. Therefore, the particle density decreases with increasing α. The error in the average potential energy per molecule is related to the approximate neglect of the last term in eq 9. It becomes more crucial for larger damping constants and smaller cutoff radii.

According to the parametrization scheme described in the previous section, the damping constant was chosen as 0.2 Å^{-1} to reach the desired 5% accuracy for both average density and energy. Then the cutoff radii were varied from 12 to 6 Å. Average potential energy and density were recorded as functions of R_C (Figures 3 and 4). The deviation of energy and density from the reference values increases for decreasing cutoff radii, as expected. However, the 5% accuracy threshold is reached at a cutoff distance of only 9 Å. The combination of $\alpha = 0.2$ Å^{-1} and $R_C = 9$ Å yielding near-Ewald quality was used in all subsequent investigations.

Radial pair distribution functions were computed according to

$$g_{ij}(r) = \frac{3}{4\pi}\left\langle \frac{n_j(r-\Delta r/2; r+\Delta r/2)}{\rho_j[(r+\Delta r/2)^3 - (r-\Delta r/2)^3]} \right\rangle_{NpT} \qquad (21)$$

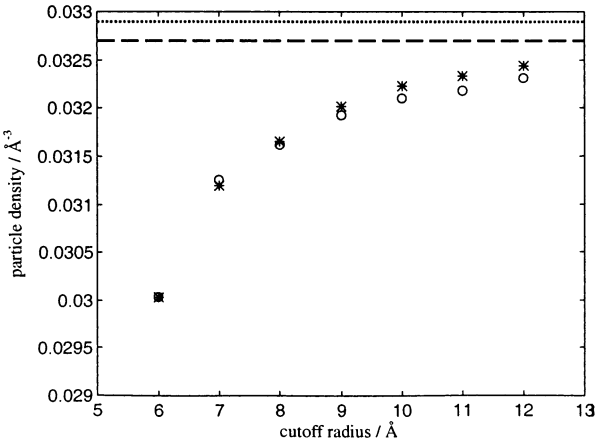

Figure 4. Average density of water molecules as a function of the cutoff radii for (○) SPC and (∗) TIP3P models. Ewald summation yields 0.0329 Å^{-3} (dashed) and 0.0327 Å^{-3} (dotted) for SPC and TIP3P water, respectively.

where r is the distance of atoms i and j, n_j is the number of atoms j within distance $r - \Delta r/2$ and $r + \Delta r/2$ of atom i with $\Delta r = 0.1$ Å, and ρ_j is the density of the atoms j. Figure 5 shows the pair distribution functions of O−O, O−H, and H−H atom pairs of SPC water model, while Figure 6 illustrates the corresponding data for TIP3P. The solid curves correspond to the damped potential and the dotted curves were obtained from simulation with Ewald summation. For comparison, we also give the corresponding distribution functions obtained with a CHARMM shifted-force potential using the same cutoff distance as for the damped Coulomb method (dashed curve). Despite the small cutoff radius of only 9 Å, our simulations using the damped potential are able to provide radial distribution functions in very close agreement with those obtained from Ewald simulations. On the other hand, the radial distribution functions taken from simulations using the standard CHARMM shifted-force potential show significantly stronger deviations from the reference data. These are particularly striking in the proximity of the cutoff radius. This is related to more pronounced perturbing effects at the cutoff distance as compared to the damped Coulomb case, thereby proving again its value.

All static properties for the final damped Coulomb parameter set and the reference simulations are summarized in Table 2. For the average potential energy, we additionally give the values obtained from constant-volume simulations at the average density of the *NpT* Ewald runs. As expected (see also ref 12), these correspond even better to the Ewald results. Note particularly for the CHARMM potential that the average density is very close to the experimental value while the average potential energy strongly deviates from the Ewald simulation data. This is related to the fact that the parametrization of the water models was done mainly with respect to experimental data by simulation with shifted-force potentials. One can therefore, on the other hand, not expect too close correspondence between Ewald simulation results and experiment.

(b) Dynamic Properties. For evaluating the dynamic properties, we first calculated the velocity autocorrelation function

$$c_v(t) = \frac{\langle \mathbf{v}_i(t)\cdot\mathbf{v}_i(0)\rangle}{\langle \mathbf{v}_i(0)\cdot\mathbf{v}_i(0)\rangle} \qquad (22)$$

where $\mathbf{v}_i$ is the velocity vector of the center of mass of water molecule i and the averages are taken over all molecules. As shown in Figure 7, excellent agreement with the reference Ewald

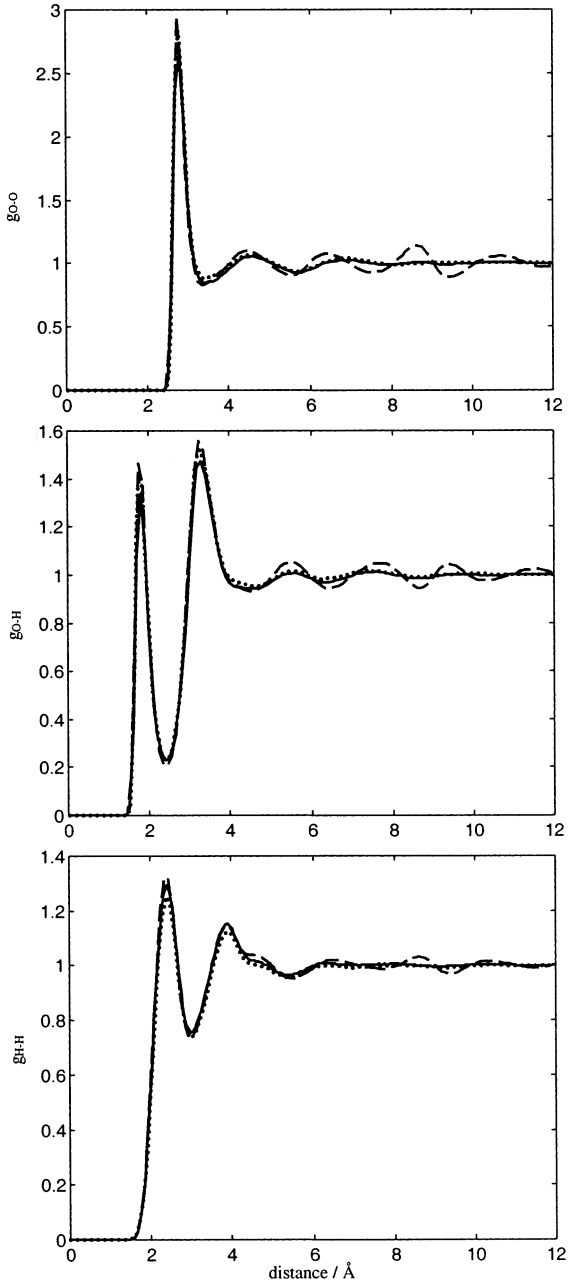

Figure 5. Pair correlation function for O−O (top), O−H (middle), and H−H (bottom) distances for SPC water using damped potential (solid), CHARMM shifted-force (dashed), and Ewald summation (dotted).

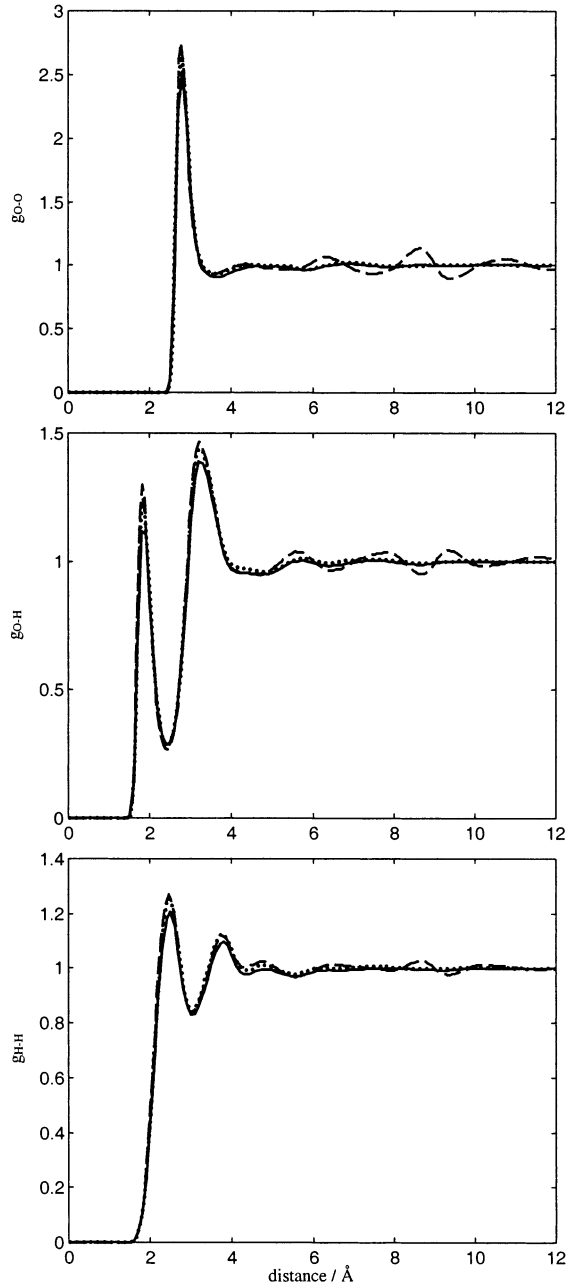

Figure 6. Pair correlation function for O−O (top), O−H (middle), H−H (bottom) distances for TIP3P water using damped potential (solid), CHARMM shifted-force (dashed), and Ewald summation (dotted).

simulations for both water models is again confirmed, whereas the CHARMM shifted-force results deviate drastically.

The diffusion constants may be calculated by integration of the velocity autocorrelation function according to

$$D = \frac{k_B T}{m} \int_0^\infty c_v(\tau)\, \mathrm{d}\tau \tag{23}$$

where m is the mass of a water molecule. Because the velocity autocorrelation function decays rapidly to zero, integration was only performed up to an upper limit of 1 ps. Table 2 shows the diffusion coefficients as obtained from simulation and from experiment. Replacing explicit Ewald summation by damped potentials yields small errors in the computation of D. The large discrepancy as compared to the experimental value is entirely due to model deficiencies. For our purposes, the correspondence between Ewald and damped Coulomb data is of importance. Again, huge deviations by using the CHARMM potential are observed. Table 2 additionally contains the relative rms fluctuations of the total energy from the *NVE* simulation runs proving stable trajectories.

(c) Dielectric Properties. Because the Q factor equals 1 for all combinations of α and R_C as discussed in section 2b, we can apply the usual relations for characterizing the dielectric behavior. The time correlation function of the total dipole moment $\mathbf{M}$

$$c_M(t) = \frac{\langle \mathbf{M}(t)\cdot\mathbf{M}(0)\rangle}{\langle \mathbf{M}(0)\cdot\mathbf{M}(0)\rangle} \tag{24}$$

for the various models is depicted in Figure 8. The correlation may be approximated by simple exponential decay according

TABLE 2: Average Potential Energy ($\langle V \rangle$), Water Density (ρ), Dielectric Permittivity (ϵ_r), Debye Relaxation Time (τ_D), Diffusion Constant (D), and Relative rms Fluctuation of the Total Energy from *NVE* Runs for SPC and TIP3P Water Models

	$\langle V \rangle$ (kcal mol^{-1})[a]	ρ (Å^{-3})	ϵ_r	τ_D (ps)	D (10^{-5} cm^2 s^{-1})	rel rms (10^{-5})
SPC_{damped}	−9.51 (−9.60)	0.0319	64	5.9	4.6	5.51
SPC_{Ewald}	−10.00	0.0327	65[24]	7.6[24]	5.8	3.02
SPC_{CHARMM}	−11.13	0.0333			2.4	4.39
$TIP3P_{damped}$	−9.05 (−9.14)	0.0320	91	6.4	6.8	9.10
$TIP3P_{Ewald}$	−9.51	0.0329	97[24], 95[25]	7.3[24], 6.1[25]	6.3	2.51
$TIP3P_{CHARMM}$	−10.60	0.0331			3.9	3.23
experiment		0.0334[23]	78.54[23]	9.3[22]	2.35[23]	

[a] Numbers in parentheses are *NVT* results at Ewald *NpT* density.

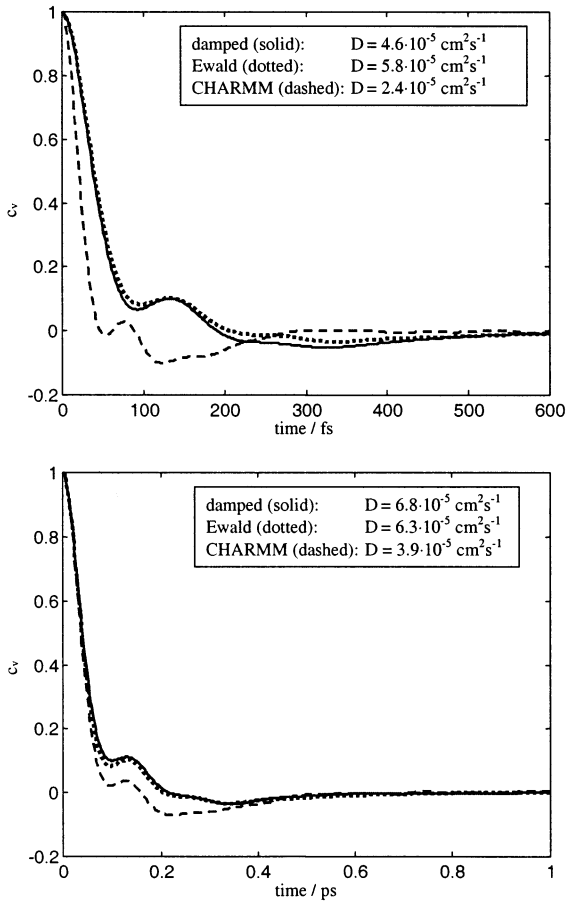

Figure 7. Velocity autocorrelation function for SPC (top) and TIP3P (bottom) water. The solid curve corresponds to damped Coulomb potential, the dotted curve was obtained from Ewald simulation, the dashed line represents the CHARMM shifted-force result.

to Debye dielectrics; the corresponding Debye relaxation times, τ_D, are listed in Table 2.

The relative dielectric permittivity, ϵ_r, was computed from the fluctuation of the total dipole moment via the Kirkwood G factor

$$G = \frac{\langle (\mathbf{M} - \langle \mathbf{M} \rangle)^2 \rangle}{N\mu^2} \tag{25}$$

as

$$\epsilon_r = 1 + 3G\frac{4\pi\rho\mu^2}{9k_BT} \tag{26}$$

where N is the total number of water molecules and μ is the dipole moment of a single water molecule. Our results are summarized in Table 2 and are compared to experiments[22,23]

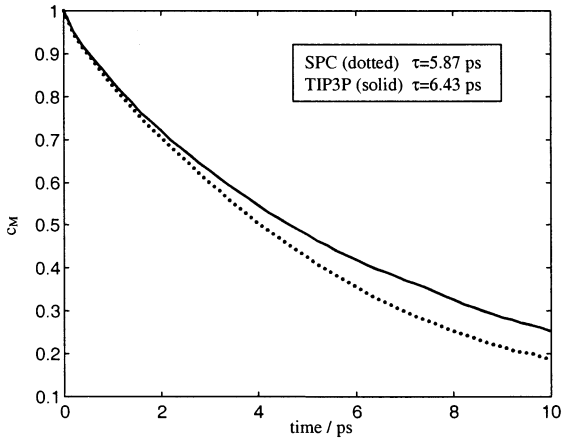

Figure 8. Dipole moment time correlation function for damped SPC (dotted) and TIP3P (solid) water models.

and to simulations of Steinhauser and co-workers[24] and of Chandra and Ichiye[25] using the Ewald summation method. Both works used the experimental water density, while we kept the system density at the value corresponding to 1 bar from earlier simulations. The deviation is however small. More significantly, while Chandra and Ichiye applied *NVE* conditions as in this work, Steinhauser and co-workers used a thermostat while sampling dynamical quantities. This affects the system dynamics dramatically. Chandra and Ichiye[25] therefore provide a much better source for comparison, though they give data for TIP3P model only. Because typical errors for the dielectric permittivity amount to roughly 5 and for the Debye relaxation times ca. 0.7 ps,[24] our results correspond to Ewald data within error bars, at least in the case of TIP3P water. However, as can be seen from the diffusion coefficients, using the damped Coulomb scheme leads to slightly slower molecular motion. There is no apparent reason for this behavior, though one might argue that the use of the damping scheme implies some loss of long-range dynamical correlation. On the other hand, we cannot rule out the possibility that the Ewald results are contaminated by artifacts due to the artificial periodicity imposed on a liquid system.

V. Conclusion

We have applied the recently introduced damped Coulomb potential to molecular dynamics simulations of SPC and TIP3P water models to demonstrate its general applicability to molecular liquids. To this end, the original theory given by Wolf et al.[10] was adapted and enhanced to yield potential and force consistency with the side effect of significant improvement of dielectric properties. With referral to Ewald summation data, the parametrization of the damping constant and cutoff radius was accomplished by a strategy that is generally transferable to other systems as well. The set of final parameters was chosen with respect to minimizing cutoff effects in a number of

observables, both static and dynamic ones. For SPC and TIP3P water, a combination of a damping constant of 0.2 $Å^{-1}$ and a cutoff distance of 9 Å was found to be appropriate. As a general result, we find that close correspondence with Ewald data is achieved at less computational cost than the Ewald scheme: with our barely optimized code, the damped Coulomb computations compared to the traditional Ewald implementation are roughly twice as fast; compared to particle-mesh Ewald,[26] the speed-up is around 25%, in line with expectations.

Static properties such as radial distribution functions were produced in excellent agreement to the reference simulations. The same applies to the average potential energy per molecule and average particle density that were the primary properties used for parametrization of damping constant and cutoff radius. As an example for the improvement over existing shifted-force schemes, we additionally applied the CHARMM function. Particularly in the cutoff distance proximity, well-known artifacts are effectively eliminated by using the damped Coulomb formalism. Furthermore, fluctuations, time correlation functions, and related data were computed. The dielectric permittivity and the Debye relaxation time of damped Coulomb simulations correspond to Ewald summation data within error bars, while the diffusion coefficients are slightly smaller in the case of the damped Coulomb potential. The deviations are more significant than those for static properties yet very small. Again, applying the CHARMM potential introduces huge deviations.

Future investigations will be dedicated to the simulation of other pure and mixed liquids, as well as solute molecules in solution, to verify the general applicability of the damped Coulomb method. Furthermore, different damping terms might be investigated with respect to computational speed and numerical accuracy. In light of the success outlined in this work, this certainly appears promising.

Acknowledgment. B.S. and D.Z. thank the Deutsche Forschungsgemeinschaft (DFG) and the DFG Graduiertenkolleg "Kinetik und Mechanismen von Ionenreaktionen" for financial support.

References and Notes

(1) Ewald, P. P. *Ann. Phys. (Leipzig)* **1921**, *64*, 253.

(2) Hummer, G.; Soumpasis, D. K. *Phys. Rev. E* **1994**, *49*, 591.

(3) van der Spoel, D.; van Maaren, P. J.; Berendsen, H. J. C. *J. Chem. Phys.* **1998**, *108*, 10220.

(4) Steinbach, P. J.; Brooks, B. R. *J. Comput. Chem.* **1994**, *15*, 667.

(5) Brooks, C. L. *J. Chem. Phys.* **1987**, *86*, 5156.

(6) Brooks, B. R.; Bruccoleri, R. E.; Olafson, B. D.; States, D. J.; Swaminathan, S.; Karplus, M. *J. Comput. Chem.* **1983**, *4*, 187.

(7) Schrimpf, G.; Schlenkrich, M.; Brickmann, J.; Bopp, P. A. *J. Phys. Chem.* **1992**, *96*, 7404.

(8) Dufner, H.; Kast, S. M.; Brickmann, J.; Schlenkrich, M. *J. Comput. Chem.* **1997**, *18*, 660.

(9) Resat, H.; McCammon, J. A. *J. Chem. Phys.* **1998**, *108*, 9617.

(10) Wolf, D.; Keblinski, P.; Phillpot, S. R.; Eggebrecht, J. *J. Chem. Phys.* **1999**, *110*, 8254.

(11) Wolf, D. *Phys. Rev. Lett.* **1992**, *68*, 3315.

(12) Demontis, P.; Spanu, S.; Suffritti, G. B. *J. Chem. Phys.* **2001**, *114*, 7980.

(13) Jorgensen, W. L.; Chandrasekhar, J.; Madura, J. D.; Impey, R. W.; Klein, M. L. *J. Chem. Phys.* **1983**, *79*, 926.

(14) Berendsen, H. J. C.; Postma, J. P. M.; van Gunsteren, W. F.; Hermans, J. In *Intermolecular Forces*; Pullman, B., Ed.; Reidel: Dordrecht, Netherlands, 1981; p 331.

(15) Neumann, M.; Steinhauser, O. *Chem. Phys. Lett.* **1983**, *95*, 417.

(16) Neumann, M. *Mol. Phys.* **1983**, *50*, 841.

(17) Smith, W.; Forester, T. *J. Mol. Graphics* **1996**, *14*, 136.

(18) Rykaert, J.-P.; Ciccotti, G.; Berendsen, H. J. C. *J. Comput. Phys.* **1977**, *23*, 327.

(19) Berendsen, H. J. C.; Postma, J. P. M.; van Gunsteren, W. F.; DiNola, A.; Haak, J. R. *J. Chem. Phys.* **1984**, *81*, 3684.

(20) Kast, S. M.; Brickmann, J. *J. Chem. Phys.* **1996**, *104*, 3732.

(21) Kast, S. M., manuscript in preparation.

(22) Hasted, J. B. In *Water: A Comprehensive Treatise*; Franks, F., Ed.; Plenum: New York, 1972; Vol. 1, Chapter 7.

(23) *CRC Handbook of Chemistry and Physics*; Lide, D. R., Ed.; CRC Press: Boca Raton, FL, 1994.

(24) Höchtl, P.; Boresch, S.; Bitomsky, W.; Steinhauser, O. *J. Chem. Phys.* **1998**, *109*, 4927.

(25) Chandra, A.; Ichiye, T. *J. Chem. Phys.* **1999**, *111*, 2701.

(26) Essmann, U.; Perera, L.; Berkowitz, M. L.; Darden, T.; Lee, H.; Pedersen, L. G. *J. Chem. Phys.* **1995**, *103*, 8577.